

Momentum-Transfer and Inelastic-Collision Cross Sections for Electrons in O₂, CO, and CO₂†

R. D. HAKE, JR.* AND A. V. PHELPS

Westinghouse Research Laboratories, Pittsburgh, Pennsylvania

(Received 20 January 1967)

Momentum-transfer and inelastic-collision cross sections for electrons in O₂, CO, and CO₂ are calculated from measured values of the electron drift velocity, characteristic energy, attachment coefficient, and ionization coefficient. The experimental data for O₂ are most consistent with vibrational excitation cross sections consisting of a series of resonances located at the vibrational energy levels of the negative ion and having values of cross section times energy half-width of the order of 10⁻¹⁸ cm² eV. The calculated effective dipole moment for rotational excitation of CO is in very good agreement with values obtained by other techniques. The vibrational excitation cross section for CO at electron energies below 1 eV is in agreement with theoretical predictions. The vibrational excitation cross sections required for consistency with the CO₂ data are very large [(2-5) × 10⁻¹⁶ cm²] and include a peak very close to the vibrational threshold of 0.083 eV.

I. INTRODUCTION

THIS paper presents the results of calculations of momentum-transfer and inelastic cross sections for electrons in O₂, CO, and CO₂ from experimentally measured values of transport coefficients. Our analyses are most accurate for the determination of the cross sections for momentum transfer and vibrational excitation in the three gases. Significant information has been obtained concerning the excitation of rotational levels in CO. Some information has also been obtained about rotational excitation in O₂ and the excitation of electronic states in O₂ and CO₂.

The present results represent an extension of previous determinations of cross sections in H₂,^{1,2} D₂,² N₂,^{1,3} and the rare gases.⁴ The technique is virtually unchanged from that described in Frost and Phelps¹ (hereafter called I) and Engelhardt and Phelps,² so that detailed discussion will be omitted. Briefly, we solve numerically the time- and space-independent Boltzmann transport equation for the distribution function of electron energies ϵ in a neutral gas using an initial set of elastic and inelastic cross sections. Transport coefficients are calculated by taking suitable averages^{1,2} over this distribution function and are compared with experimental values of the same transport coefficients. The initial cross sections are then successively modified and the procedure is repeated in order to obtain better agreement with the experimental transport coefficients. The cross sections are considered satisfactory when our calculated values match the experimental values to

within 5% over an extended range of the ratio of the electric field strength E to gas density N .

Two methods of solving the Boltzmann equation are discussed in the Appendix of I: (a) an "exact" solution for field strengths which are low enough such that the electrons are near thermal equilibrium (so that it is necessary to consider collisions of the second kind, i.e., superelastic collisions), and (b) a solution neglecting collisions of the second kind. Most of our present calculations have employed the latter solution. However, when considering ϵ_K values close to kT it is necessary to include collisions of the second kind. Here $\epsilon_K = eD/\mu$ is the characteristic energy of the electrons, e is the electronic charge, D and μ are the electron diffusion and mobility coefficients, k is the Boltzmann constant, and T is the gas temperature. In the case of CO₂, rotational excitation appears to be unimportant for the available experimental data, so that the exact solution involves only a small number of vibrational levels and is readily carried out. In the cases of O₂ and CO, an exact solution would include approximately as many rotational levels as previously^{1,3} required for N₂ and would be valid only over a very limited range of ϵ_K/kT for $T \leq 77^\circ\text{K}$. In Appendix A we develop an approximate solution for low values of ϵ_K/kT in which the effect of the many rotational energy levels is approximated by a single rotational level with a threshold and a magnitude which gives results consistent with the continuous approximation of I at large values of ϵ_K/kT . This approximation is used in our calculations for O₂ and CO at low ϵ_K/kT .

As in previous analyses¹⁻⁴ we have facilitated the cross-section determinations by employing two combinations of measured transport coefficients: (a) the momentum-transfer collision frequency ν_m which is defined by

$$\nu_m/N = (e/m)E/Nw, \quad (1)$$

and which is primarily sensitive to the cross section for momentum transfer, and (b) the energy exchange collision frequency ν_u which is defined by

$$\nu_u/N = ew(E/N)/(\epsilon_K - kT), \quad (2)$$

† This work was supported in part by the Air Force Weapons Laboratory, Research and Technology Division, Air Force Systems Command, U. S. Air Force, Kirtland Air Force Base, New Mexico, and by Project Defender, sponsored by the Advanced Research Projects Agency, Department of Defense.

* Present address: The University of Pittsburgh, Pittsburgh, Pennsylvania.

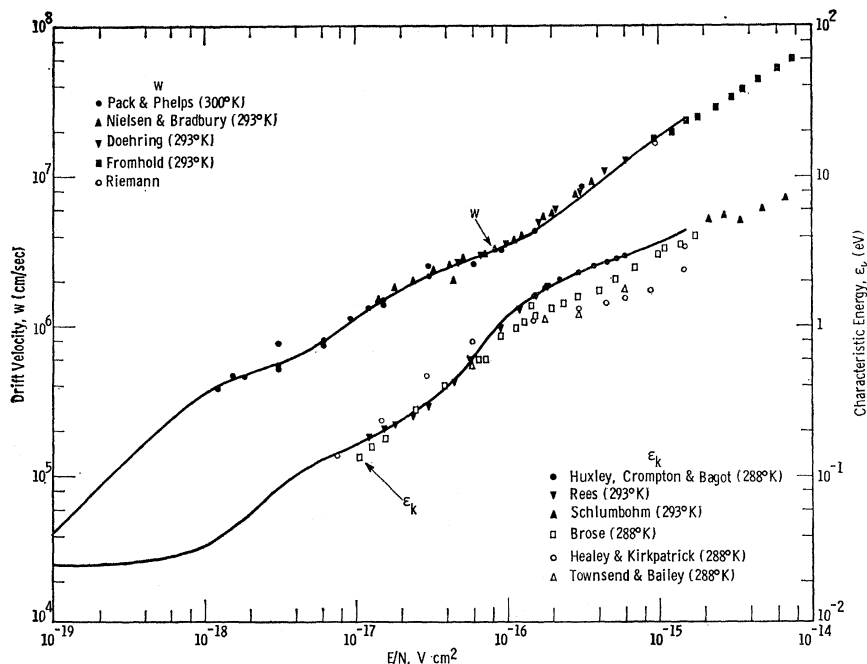
¹ L. S. Frost and A. V. Phelps, Phys. Rev. **127**, 1621 (1962).

² A. G. Engelhardt and A. V. Phelps, Phys. Rev. **131**, 2115 (1963).

³ A. G. Engelhardt, A. V. Phelps, and C. G. Risk, Phys. Rev. **135**, A1566 (1964).

⁴ L. S. Frost and A. V. Phelps, Phys. Rev. **136**, A1538 (1964).

FIG. 1. Experimental and theoretical drift velocities and characteristic energies for electrons in oxygen. A smooth curve (not shown) through the w and ϵ_K data shown by the solid points was used to construct the ν_m/N and ν_u/N curves of Fig. 2. The solid curves shown are the results of the calculations using the cross sections of Figs. 4-6.



and which is primarily sensitive to the inelastic cross sections. Here m is the mass of the electron and w is the electron drift velocity.

The details of the determinations of the momentum transfer and inelastic cross sections for O_2 , CO , and CO_2 are given in Secs. II, III, and IV, respectively.

II. OXYGEN

The determination of elastic- and inelastic-scattering cross sections for electrons in oxygen is of particular interest because of the importance of oxygen in the ionosphere. The experimental⁵⁻¹⁶ values of the dc transport coefficients w and ϵ_K are shown as points in Fig. 1. As suggested by the limited range of the ϵ_K values and the large scatter in the data, the measurements of transport coefficients in O_2 is considerably more difficult than in nonattaching gases such as N_2 and H_2 . We have based our analysis on the more recent results^{12,14,15} for

⁵ H. L. Brose, *Phil. Mag.* **50**, 536 (1925).

⁶ V. S. Townsend and V. A. Bailey, *Phil. Mag.* **42**, 873 (1921).

⁷ R. A. Nielsen and N. E. Bradbury, *Phys. Rev.* **51**, 69 (1937).

⁸ R. H. Healey and C. B. Kirkpatrick, as given in R. H. Healey and J. W. Reed, *The Behavior of Slow Electrons in Gases* (Amalgamated Wireless, Inc., Sydney, Australia, 1941), p. 94.

⁹ W. Riemann, *Z. Physik* **122**, 216 (1944).

¹⁰ A. Doehring, *Z. Naturforsch.* **7**, 253 (1952).

¹¹ M. A. Harrison and R. Geballe, *Phys. Rev.* **91**, 1 (1953).

¹² L. G. H. Huxley, R. W. Crompton, and C. H. Bagot, *Australian J. Phys.* **12**, 303 (1959).

¹³ L. Frommhold, *Fortschr. Physik* **12**, 597 (1964). In the present analysis we assume that the results of Refs. 17-19 for α_a/N and α_i/N at $E/N < 10^{-16}$ V cm² are obtained under conditions such that the detachment observed by Frommhold is not significant.

¹⁴ H. Schlumbohm, *Z. Physik* **184**, 492 (1965).

¹⁵ J. A. Rees, *Australian J. Phys.* **18**, 41 (1965).

¹⁶ J. L. Pack and A. V. Phelps, *J. Chem. Phys.* **44**, 1870 (1966); **45**, 4316 (1966).

ϵ_K and have used these to construct the solid curves of ν_m/N and ν_u/N of Fig. 2. Unfortunately, the use of ν_m/N and ν_u/N does not result in as complete a separation of the effects of elastic and inelastic collisions for O_2 as is the case for H_2 , N_2 , and CO . We also make use of the recent measurements of two-body electron attachment coefficients,^{12,17-20} α_a/N , and the difference between first Townsend ionization coefficient,¹⁷⁻¹⁹ α_i/N , and α_a/N as shown by the points in Fig. 3. The cross sections required to fit the measured transport coefficients are shown in Figs. 4 to 6. The smooth curves of Fig. 1 and the points of Fig. 2 show the transport coefficients calculated using these cross sections. As suggested by the structure in the ν_u/N curve of Fig. 2, it is convenient to divide our discussion into a low-energy region, $\epsilon_K < 1.0$ eV, and a moderate-energy region, 1.0 eV $< \epsilon_K < 3.0$ eV.

A. Low Energies ($\epsilon_K < 1.0$ eV, $E/N < 10^{-16}$ V cm²)

In the low-energy region the important inelastic-collision processes in O_2 are rotational excitation, vibrational excitation, and, possibly, electronic excitation of the $a^1\Delta_g$ and $b^1\Sigma_g^+$ levels with thresholds at 0.98 and 1.63 eV, respectively. This is also the range of energies for which electron attachment occurs predominantly by the three-body process.^{20,21} Since ϵ_K measurements are

¹⁷ A. N. Prasad and J. D. Craggs, *Proc. Phys. Soc. (London)* **78**, 385 (1961).

¹⁸ J. Dutton, F. Llewellyn-Jones, and G. B. Morgan, *Nature* **198**, 680 (1963).

¹⁹ J. B. Freely and L. H. Fisher, *Phys. Rev.* **133**, A304 (1964).

²⁰ L. M. Chanin, A. V. Phelps, and M. A. Biondi, *Phys. Rev.* **128**, 219 (1962).

²¹ G. J. Schulz, *Bull. Am. Phys. Soc.* **6**, 387 (1961).

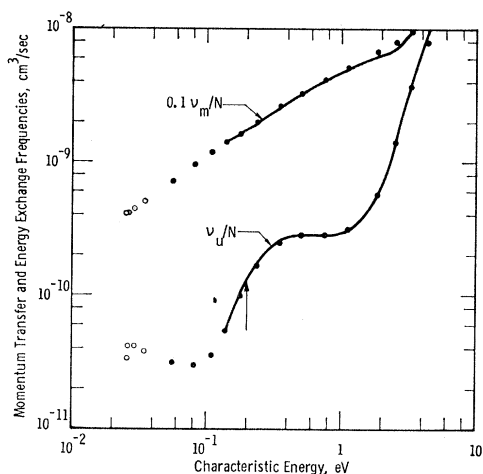


FIG. 2. Momentum-transfer and energy-exchange collision frequencies per molecule for electrons in oxygen. The solid curves are calculated from the experimental data of Fig. 1. The solid circles are calculated using the excitation cross sections discussed in the text and the continuous approximation to rotational excitation. The open circles were calculated using the single-level approximation to rotational excitation as discussed in the text. The arrow indicates the value of ϵk equal to the lowest threshold energy for vibrational excitation.

not available below 0.15 eV and since the threshold for vibrational excitation is 0.195 eV, we will obtain very little information about rotational excitation. Also, since electron-beam studies in this energy range²² yield only the integrated values of the excitation cross sections near threshold and since there are no theoretical cross sections for vibrational or electronic excitation, we are faced with an infinity of possible choices.

It appears that the assumption which is most consistent with all of the available experimental data is that the vibrational excitation cross sections consist of

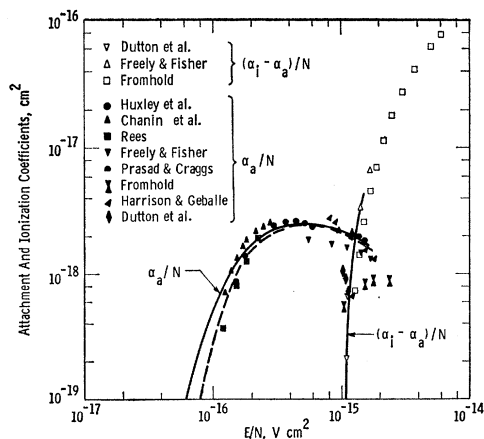


FIG. 3. Experimental and theoretical attachment and ionization coefficients for electrons in oxygen. The solid and open points give measured values of α_a/N and $(\alpha_i - \alpha_a)/N$, respectively. The curves are the results of our calculations using the cross sections discussed in the text.

²² G. J. Schulz and J. T. Dowell, *Phys. Rev.* **128**, 174 (1962).

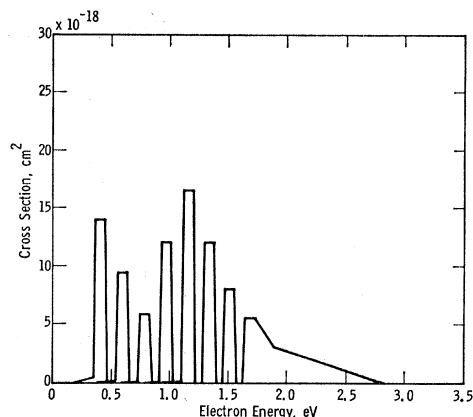


FIG. 4. Vibrational excitation cross sections for electrons in O_2 derived from experimental data of Figs. 1 and 2. The delay between the various thresholds and the beginning of the corresponding resonance is assumed equal to the "well depth" used in Ref. 22, i.e., 0.16 eV. The initial slopes of the various cross sections were adjusted to be consistent with this reference.

a set of narrow spikes delayed in energy relative to the vibrational excitation thresholds.²²⁻²⁴ This assumption is consistent with the small values of the integrated cross sections near threshold measured by Schulz and Dowell²² and with the large cross sections required to explain the values of ν_u/N shown in Fig. 2. If the set of resonant-type cross sections is assumed to be connected with the formation of short-lived vibrational states of the ${}^2\Pi_g$ ground state of the O_2^- ion, then the assumptions

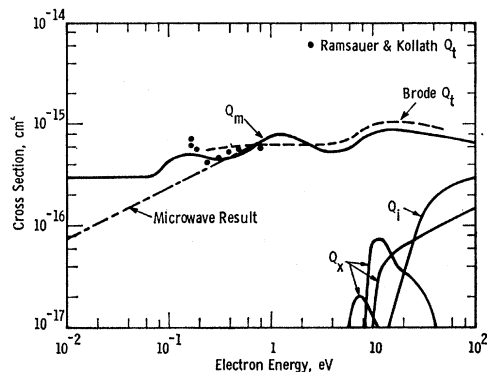


FIG. 5. Momentum-transfer Q_m and inelastic cross sections Q_x for electrons in O_2 derived from experimental ν_m/N and ν_u/N data. The ionization cross section Q_i is taken from Tate and Smith. The results of electron-beam measurements of the total scattering cross section Q_t of Ramsauer and Kollath and of Brode are shown by the points and the dashed line. Also shown is the energy-dependent momentum-transfer cross section derived from microwave experiments.

²³ This assumption is rather different from that used in an earlier attempt to analyze O_2 data. See A. V. Phelps, *Natl. Bur. Std. (U. S.) Tech. Notes* **211**, Vol. 5, 49 (1964).

²⁴ M. J. W. Boness and J. B. Hasted, *Phys. Letters* **21**, 526 (1966). Note that the close spacing of the resonances found by these authors (~ 0.11 eV) appears inconsistent with the spacing required (~ 0.19 eV) to explain the small cross sections observed in Ref. 22. The closer spacing agrees with the theory of P. E. Cade, *Bull. Am. Phys. Soc.* **11**, 42 (1966).

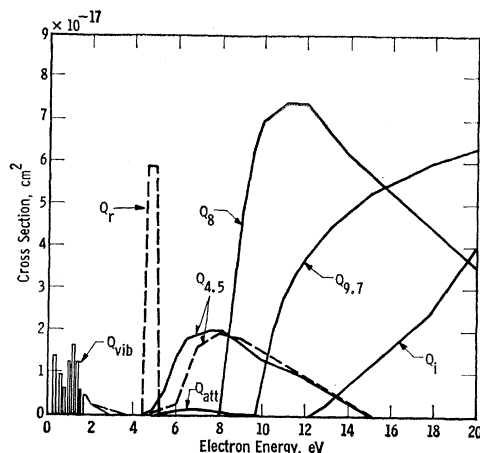


FIG. 6. Inelastic-collision cross sections for electrons in O_2 derived from transport coefficients. The subscripts to the Q 's indicate the process involved. Thus, $Q_{4.5}$ is the excitation cross section for the $A^3\Sigma_u^+$ level with a threshold at 4.5 eV while Q_{att} is the dissociative-attachment cross section from electron-beam experiments.

are consistent with structure observed by Schulz²¹ in the energy dependence of three-body attachment coefficient. A series of resonant-type peaks has recently been observed in the total cross section by Boness and Hasted.²⁴ Although it is possible that the capture of an electron into any one of the temporary negative-ion states will be followed by autodetachment and excitation of any of the energetically available vibrational states, as in nitrogen,²⁵ we have no experimental or theoretical basis for assigning the relative magnitudes of vibrational excitation cross sections. We will therefore assign the total magnitude of the resonant-type cross section to the vibrational state having its threshold just below the resonance. These cross sections are shown in Fig. 4. The derived cross sections will therefore be equal to or larger than the sum of the true cross sections. The widths in energy of the cross sections shown in Fig. 4 are chosen for computational convenience and only their integrated magnitudes are expected to be significant, i.e., only the magnitudes of the resonant portions of the cross sections were adjusted during the calculations. Therefore, Fig. 4 is more properly interpreted as showing that the integral of the cross section over energy for the first resonant peak, for example, is approximately $1.4 \times 10^{-18} \text{ cm}^2 \text{ eV}$. We have not investigated the effect of large changes in the shapes of the resonances on the calculations.

Our assignment of all of the inelastic cross section for electron energies between 0.9 and 4.4 eV to vibrational excitation is rather arbitrary in view of the possible excitation of the $a^1\Delta_g$ and $b^1\Sigma_g^+$ states. In fact, the increase in the derived cross sections for energies above 0.98 eV suggests that new modes of excitation, e.g., $a^1\Delta_g$ excitation, are important. We do not know whether the resonance type of excitation is applicable to the

²⁵ G. J. Schulz, Phys. Rev. **125**, 229 (1962); **135**, A988 (1964).

excitation of the $a^1\Delta_g$ and $b^1\Sigma_g^+$ levels. An additional complication which we have not taken into account is the possibility that there are resonances due to other electronic states of the negative ion, e.g., vibrational levels of the $^4\Sigma_g^-$ state of O_2^- . If we were to assume a set of resonant cross sections located at the vibrational excitation thresholds of the $X^3\Sigma_g^-$ ground state of the neutral molecule instead of the delayed resonances shown in Fig. 4, then the magnitude of the lowest energy peak would be lowered by a factor of approximately 6. The magnitude of the higher-energy resonances would approach the values shown in Fig. 4. If, as suggested by the recent results of Boness and Hasted,²⁴ the separation of the inelastic resonances is less than we have assumed, then the integrated magnitudes of each vibrational cross section would be smaller than the values shown.

The cross section for momentum transfer collisions, Q_m , for oxygen obtained from our analysis is shown in Fig. 5. When this cross section is combined with the vibrational excitation cross sections of Fig. 4 and with a set of rotational excitation cross sections calculated from the theory of Gerjuoy and Stein²⁶ using an effective quadrupole moment of $1.8ea_0^2$, we obtain the set of ν_m/N and ν_u/N values shown by the solid circles of Fig. 2 and the values of w and ϵ_K shown by the solid line of Fig. 1. Thus, we are able to obtain good agreement with an average of the experimental values of ν_m/N and ν_u/N shown by the solid curve of Fig. 2. The portion of the $Q_m(\epsilon)$ curve shown in Fig. 5 below 0.1 eV is chosen to give a reasonable fit to the values for the mobility of thermal electrons in O_2 obtained by Pack and Phelps¹⁶ from measurements in O_2 - CO_2 mixtures. The effective quadrupole moment was then chosen to obtain agreement between the calculated and experimental drift velocities for $10^{-18} < E/N < 2 \times 10^{-17} \text{ V cm}^2$.

Much lower values of Q_m have been obtained for near thermal electrons in O_2 from microwave conductivity data by van Lint, Wikner, and Trueblood,²⁷ by Fehsenfeld,²⁸ by Mentzoni,²⁹ and by Veach, Verdeyen, and Cahn.³⁰ The $Q_m(\epsilon)$ curve derived from the microwave results of Mentzoni and of Veach *et al.* is shown dashed in Fig. 5 and is designated "Microwave Results." The electron mobility inferred by Pack and Phelps from attachment-detachment equilibrium studies¹⁶ at 544°K is consistent with the microwave results. On the other hand, the high-frequency conductivity data of Carruthers³¹ is consistent with values of Q_m reasonably close to the values given by the solid curve of Fig. 5. All of

²⁶ E. Gerjuoy and S. Stein, Phys. Rev. **97**, 1671 (1955); **98**, 1848 (1955).

²⁷ V. A. J. van Lint, E. G. Wikner, and D. L. Trueblood, Bull. Am. Phys. Soc. **5**, 122 (1960). See also General Atomic Division of General Dynamics Corporation Report GACD-2461, 1961, San Diego, California (unpublished).

²⁸ F. C. Fehsenfeld, J. Chem. Phys. **39**, 1653 (1963).

²⁹ M. H. Mentzoni, J. Res. Natl. Bur. Std. (U. S.) **69D**, 213 (1965).

³⁰ G. E. Veatch, J. T. Verdeyen, and J. H. Cahn, Bull. Am. Phys. Soc. **11**, 496 (1966).

³¹ J. A. Carruthers, Can. J. Phys. **40**, 1528 (1962).

these low-energy values of Q_m are much lower than those of Heylen.³² If the microwave results are correct, then it will be necessary to increase the energy losses near the onset of vibrational excitation by about a factor of 2. One conceivable way to make the microwave results consistent with the drift velocities of Fig. 1 for $E/N \sim 2 \times 10^{-17}$ V cm² is to assume a resonance peak³³ in the $Q_m(\epsilon)$ curve at about 0.15 eV. Possible evidence for such a peak was found by Ramsauer and Kollath.³⁴ This peak is expected to be due to the same compound state as that proposed to explain the three-body attachment of electrons^{20,21} at energies below 0.2 eV. This possibility needs to be investigated further.

The effective quadrupole moment of $1.8ea_0^2$ used to fit the drift velocity data at low E/N is to be compared with an upper limit of $0.4ea_0^2$ obtained from microwave studies of line broadening.³⁵ Evidence for a large effective quadrupole moment has recently been obtained by Mentzoni and Narasinga Rao³⁶ from measurements of the decay of electron energy during the afterglow of a discharge in oxygen. However, Geltman and Takayanagi³⁷ have concluded that short-range forces lead to cross sections for rotational excitation in oxygen which differ greatly in shape and are significantly larger at the higher electron energies than those calculated using the Gerjuoy and Stein²⁶ relations and measured quadrupole moments. We have not yet used these cross sections in our calculations. The use of such cross sections would lead to ν_u/N values considerably below those shown by the points of Fig. 2 for $\epsilon_K < 0.1$ eV. A second possible source of large rotational excitation cross sections at energies near 0.15 eV is the resonance associated with the vibrational state of the O_2^- ion at electron energies below 0.195 eV. Such an effect has been proposed by Chen³⁷ for N_2 at energies near 2 eV. Note that the loss of electrons by the three-body attachment process should be included in the Boltzmann equation for oxygen densities above 5×10^{18} cm⁻³.

³² A. E. D. Heylen, Proc. Phys. Soc. (London) **79**, 284 (1962).

³³ If we assume the presence of a narrow resonance in the elastic-scattering cross section at about 0.15 eV and assume that this peak corresponds to the temporary excitation of a vibrational level of the $^2\pi_g$ state of the O_2^- ion, then detailed balancing arguments give a maximum cross section of $8\pi/3k^2 = 2 \times 10^{-14}$ cm², where k is the electron wave number. The integrated elastic-scattering cross section is estimated to be 2×10^{-17} cm² eV by assuming that the contribution of the resonance is such as to cause the increase in the elastic-scattering cross section near 0.15 eV to the value of Q_m given in Fig. 5. The ratio of the integrated cross section to the peak cross section gives a width of 10^{-3} eV corresponding to a lifetime of $\sim 10^{-12}$ sec. The arguments presented here are a refinement of the estimate of the lower limit to the temporary negative-ion lifetime given in footnote 28 of Ref. 20.

³⁴ C. Ramsauer and R. Kollath, Ann. Physik **4**, 91 (1930).

³⁵ W. V. Smith and R. Howard, Phys. Rev. **79**, 132 (1950).

³⁶ M. H. Mentzoni and K. V. Narasinga Rao, Phys. Rev. Letters **14**, 779 (1965).

³⁷ S. Geltman and K. Takayanagi, Phys. Rev. **143**, 25 (1966); J. C. Y. Chen, *ibid.* **146**, 61 (1966). See also K. Takayanagi, Rept. Ionosphere Space Res. Japan **19**, 1 (1965); and Y. D. Oksyuk, Zh. Eksperim. i Teor. Fiz. **49**, 1261 (1965) [English transl.: Soviet Phys.—JETP **22**, 873 (1965)].

B. Moderate Energies ($1.0 < \epsilon_K < 3.0$ eV)

The electronic excitation and ionization cross sections used to fit the measured transport coefficients are shown in Fig. 6. We will discuss the cross sections shown by the solid curves first. The dashed curves will be considered near the end of this subsection. The thresholds for the three excitation cross sections, i.e., 4.5, 8.0, and 9.7 eV, were taken from the data of Schulz and Dowell.²² The magnitudes and energy dependence of the cross sections were adjusted to fit the ν_u/N and ionization coefficient curves. As pointed out by Schulz and Dowell, the apparent thresholds at 4.5 and 8.0 eV correspond to expected appearance potentials for the $A^3\Sigma_u^+$ and $B^3\Sigma_u^-$ levels, respectively. The threshold at 9.7 eV is a rather arbitrary choice from among the large amount of structure observed in the trapped-electron experiments²² at energies above about 8.5 eV.

For ϵ_K values between 0.6 and 2.5, the 4.5-eV process had a greater effect on the ν_u/N curve than any other individual cross section, and for ϵ_K values from 1.0 to 2.5 eV at least half the total ν_u value was due to this level. Consequently, we expect the rising portion of that cross-section curve to be quite accurate provided that the inelastic cross sections in this energy range can be represented by a single cross section for a process in which the electron loses essentially all of its energy on each inelastic collision (see below). The falling portion of the 4.5-eV process cannot be considered too accurate because of the importance of the 8-eV process and because of the inherent insensitivity of our technique for inelastic cross sections which decrease with increasing electron energy.

The magnitude of the process with threshold at 8.0 eV was adjusted to give a fit to the portion of the ν_u/N curve for ϵ_K above 2 eV. Using Tate and Smith's³⁸ ionization cross section, the magnitude of the 9.7-eV process was adjusted to give a fit to the $(\alpha_i - \alpha_a)/N$ data of Freely and Fisher¹⁹ and of Dutton, Llewlyn-Jones, and Morgan,¹⁸ shown in Fig. 3. The α_a/N and α_i/N values were calculated from their respective cross sections using Eqs. (10) of Ref. 2. We have used $(\alpha_i - \alpha_a)/N$ rather than α_i/N since there is generally better agreement between experimental determinations of this quantity. This remark does not apply to the $(\alpha_a - \alpha_i)/N$ data of Fromhold,¹³ since his experiment is quite different. The same transport coefficients could probably have been obtained by reducing the 9.7-eV cross section and then adding a significant high-energy portion to the 8.0-eV process as suggested by the results of Lassetre, Silverman, and Krasnow³⁹ or by adding cross sections corresponding to lower or higher thresholds. This illustrates the point that the weighted sum of our results above 8 eV should be considered more significant than the individual cross sections. We have

³⁸ J. T. Tate and P. T. Smith, Phys. Rev. **39**, 270 (1932).

³⁹ E. N. Lassetre, S. M. Silverman, and M. E. Krasnow, J. Chem. Phys. **40**, 1261 (1964).

not attempted to fit the α_i/N and α_a/N data for $E/N > 1.5 \times 10^{-15}$ V cm², since for these higher E/N the energy required to bring the electrons produced by ionizing collisions up to the mean electron energy can no longer be neglected and since we expect poor convergence of the spherical harmonic expansion of the electron energy distribution used in our analysis.^{2,14}

The calculated attachment coefficients are shown by smooth curves in Fig. 3 where they may be compared with some of the recent experimental data shown by the solid points. The dissociative attachment cross section given by Schulz⁴⁰ was used with the cross sections shown by the solid curves of Fig. 6 to calculate the α_a/N values shown by the solid curve of Fig. 3. We see that while the agreement with most of the experimental data is satisfactory for $E/N > 1.5 \times 10^{-16}$ V cm², the calculated curve appears to increase too slowly with E/N at low E/N . A change⁴¹ in the "threshold" of the attachment cross section from 4.4 to 4.9 eV produced little change in the calculated α_a/N curve for $E/N < 10^{-16}$ V cm². At present it does not appear possible to fit the rise in α_a/N with E/N found by Frommhold at high E/N and remain consistent with the attachment cross section of Schulz and others and the ϵ_K data of Huxley, Crompton, and Bagot.⁹ Similarly, the rapid decrease in α_a/N with E/N found by Dutton, Llewlyn-Jones, and Morgan¹⁸ would appear to be very difficult to fit theoretically.

In an effort to obtain better agreement with the experimental α_a/N data while retaining agreement with the ν_m/N and ν_u/N data, we have postulated the existence of a resonance-type inelastic cross section between 4.5 and 5.0 eV. In order for such a resonance not to have been observed by Schulz and Dowell²² the electrons must lose only a fraction of their energy at threshold, i.e., the inelastic collisions result in either vibrational excitation²⁵ as in N₂ or excitation of the $a^1\Delta_g$ and/or $b^1\Sigma_g^+$ states. Since no resonance is observed in the total cross section^{34,42} or in the dissociative attachment cross section⁴⁰ in this energy range, Schulz suggests that this model requires that most of the excited molecules decay to the $a^1\Delta_g$ and/or $b^1\Sigma_g^+$ levels. Accordingly, we have assumed that the effective energy loss due to excitation via the resonance is 1.0 eV. As in the case of N₂, the effect of such a resonance is to cause a rapid drop in the electron energy distribution function at energies near the resonance. The cross sections and attachment coefficients derived using this model are shown by the dashed curves of Figs. 3 and 6. The values of w , ϵ_K , ν_m/N , ν_u/N , and $(\alpha_a - \alpha_i)/N$ calculated using

this model agree with those calculated above and with experiment to within 5%. Experiments to test this model are essential at this stage.

The Q_m curve obtained from our analysis for ϵ_K between 1 and 3 eV and shown in Fig. 5 is slightly lower than the total cross section given by Brode⁴² and shows a maximum at about 1.3 eV which is not present in the Q_t data. We note that the experimental values of ν_m/N are about 10% lower than the calculated values for $\epsilon_K \sim 2.5$ eV. Our results are in reasonable agreement with those of Heylen³² for energies above about 0.5 eV.

C. Application to Dry Air

Figure 7 shows a comparison of ν_m/N and ν_u/N values for dry air as calculated from available^{7,9,43-45} experimental data and as calculated using the cross sections for electrons in O₂ given in Figs. 4-6 and cross sections found previously for nitrogen.³ We see that the calculated points agree with the smooth curve based on experiment to within 20%. While this agreement indicates that the calculated transport coefficients would be satisfactory for most applications, e.g., the w and ϵ_K values agree with experiment to within 10%, the discrepancy is much larger than for either pure gas. It

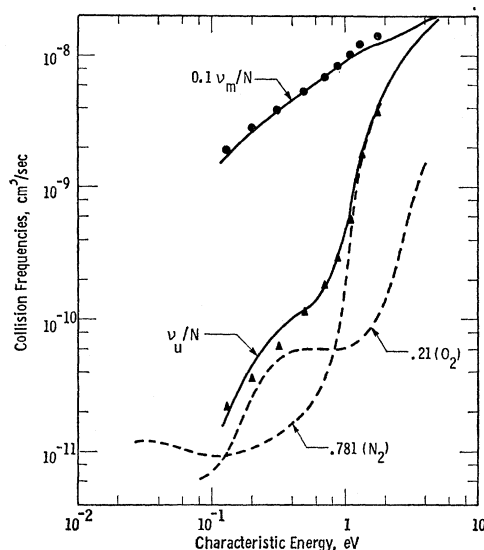


Fig. 7. Momentum-transfer and energy-exchange collision frequencies per molecule for electrons in air. The solid curves are computed from smooth curves through the experimental values of w as given by Nielsen and Bradbury and the experimental values of ϵ_K as given by Crompton, Huxley, and Sutton and by Rees and Jory. The points show the values of ν_m/N and ν_u/N calculated using the cross sections derived in this paper for O₂ and the cross sections derived by Engelhardt, Phelps, and Risk for N₂. The dashed curves show the ν_u/N values for pure O₂ and N₂ multiplied by their respective fractional concentrations, i.e., 21 and 78.1%, respectively.

⁴⁰ G. J. Schulz, Phys. Rev. **128**, 178 (1962).

⁴¹ According to L. G. Christophorou, R. N. Compton, G. S. Hurst, and P. W. Reinhardt [J. Chem. Phys. **43**, 4273 (1965)] such a shift in threshold gives good agreement between calculated and measured attachment coefficients in O₂-Ar mixtures. Since the range of mean electron energies covered in their experiments is very small, i.e., 2.3 to 3.0 eV, the analysis depends critically on the shape of the cross section determined by electron-beam techniques.

⁴² R. B. Brode, Rev. Mod. Phys. **5**, 257 (1933). This paper summarizes results obtained by previous investigators.

⁴³ J. S. Townsend and H. T. Tizard, Proc. Roy. Soc. (London) **A88**, 336 (1913).

⁴⁴ R. W. Crompton, L. G. H. Huxley, and D. J. Sutton, Proc. Roy. Soc. (London) **A218**, 507 (1953).

⁴⁵ J. A. Rees and R. L. Jory, Australian J. Phys. **17**, 307 (1964).

appears that either the experimental data used in our analyses for one or more of the gases are in error or that the lack of uniqueness in the choice of vibrational excitation cross sections for O_2 leads to error when the same cross sections are used for air.

The dashed curves of Fig. 7 show the ν_u/N values appropriate to the fractional concentration of N_2 and O_2 in air, i.e., 78.1 and 21% of the pure N_2 and O_2 values, respectively. The sum of the dashed curves should be roughly equal to the solid ν_u/N curve. This comparison is very approximate because of changes in the electron-energy distribution functions, but does show that in spite of the low concentration of O_2 , vibrational excitation of O_2 is the dominant energy-loss mechanism in air for characteristic energies between 0.13 and 0.8 eV corresponding to electron energies between 0.195 and 1.7 eV. As yet we have not made a detailed comparison of measured attachment and ionization coefficients for air with those calculated using the O_2 and N_2 data.

The preceding analysis has neglected the contribution of the vibrational excitation of CO_2 to the electron-energy losses in air of standard sea-level composition because this effect is expected to be significant only for ϵ_K below about 0.2 eV. Using the ν_m/N data of Sec. IV, one expects the contribution of the 0.03% CO_2 to be 1–2% of the sum of the N_2 and O_2 contributions for thermal electrons at $T < 300^\circ K$. The contribution of CO_2 to ν_u/N is 5–10% for $\epsilon_K < 0.08$ eV and less for higher ϵ_K . The contribution of the 0.9% Ar present in air to ν_m/N and ν_u/N is expected to be less than 1% at all ϵ_K . The presence of small amounts of H_2O in air, e.g., 1%, can cause large changes in the electron transport coefficients from those for dry air at low ϵ_K . A consistent set of elastic and inelastic cross sections for electrons in H_2O has been obtained from transport-coefficient data and will be published elsewhere.

III. CARBON MONOXIDE

The determination of elastic and inelastic scattering cross sections for low-energy electrons in CO is of particular interest because of recent theoretical calculations^{46–49} of these cross sections for molecules with a permanent dipole moment. Fortunately, there is recent experimental transport coefficient data^{50,51} in the low- ϵ_K

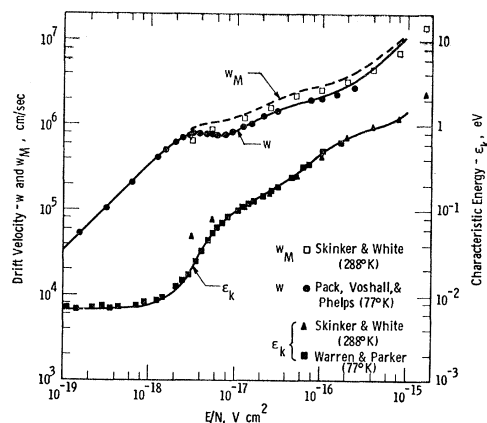


Fig. 8. Drift velocities and characteristic energy for electrons in CO as a function of E/N . The points show the experimental data and the smooth curves show the coefficients calculated using the cross sections of Figs. 10 and 11. As indicated in the text, no attempt was made to adjust the cross sections for energies above 1 eV so as to obtain a fit of the curves of w , w_M , and ϵ_K to the experimental data for $E/N > 10^{-16}$ V cm².

region for which the theory applies. Also, the type of analysis presented in this paper appears to be particularly appropriate for CO at low ϵ_K , i.e., a good separation between elastic and inelastic effects is achieved using the ν_m/N and ν_u/N coefficients. The experimental values^{50–53} of w and ϵ_K are shown by the solid points in Fig. 8. A smooth curve (not shown in Fig. 8) through these points is used to calculate the solid curves of ν_m/N and ν_u/N in Fig. 9. Because of the limited range

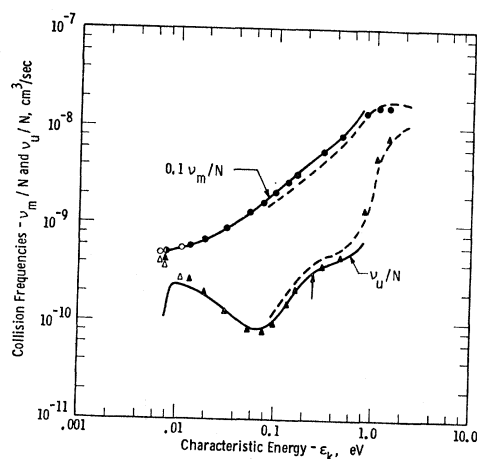


Fig. 9. Effective collision frequencies for momentum-transfer and energy-exchange collisions per molecule for electrons in CO. The smooth curves were calculated from smooth curves through the experimental data of Fig. 8. The points were calculated using the cross sections given in Figs. 10 and 11. The open and closed points were obtained using 16 rotational levels and the continuous approximation, respectively. The arrow indicates a value of ϵ_K equal to the lowest threshold for vibrational excitation.

⁴⁶ S. Altschuler, Phys. Rev. **107**, 114 (1957).

⁴⁷ K. Takayanagi, J. Phys. Soc. Japan **21**, 507 (1966). This reference gives corrected and generalized forms of relations for rotational excitation desired by H. S. W. Massey [Proc. Cambridge Phil. Soc. **28**, 99 (1932)] and generalizes the formula for vibrational excitation from the lowest rotational level given by T. Y. Wu [Phys. Rev. **71**, 111 (1947)].

⁴⁸ M. H. Mittelman and R. E. von Holdt, Phys. Rev. **140**, A726 (1965).

⁴⁹ E. L. Breig and C. C. Lin, Phys. Rev. **43**, 3839 (1965). We note that in the case of N_2 , these authors use an approach which is very different from that used by J. C. Y. Chen, J. Chem. Phys. **40**, 3513 (1964). The latter theory has been found to agree well with the experiment (Ref. 3).

⁵⁰ J. L. Pack, R. E. Voshall, and A. V. Phelps, Phys. Rev. **127**, 2084 (1962).

⁵¹ R. W. Warren and J. H. Parker, Jr., Phys. Rev. **128**, 2661 (1962).

⁵² M. F. Shinker and J. V. White, Phil. Mag. **46**, 630 (1923).

⁵³ We have not plotted the time-of-flight drift velocity data of H. B. Wahlin [Phys. Rev. **35**, 1568 (1930)], since the values are impossibly high, probably due to impurities such as CO_2 .

of E/N for which the time-of-flight drift velocity w data are available we have also used the magnetic drift velocity^{8,54} w_M data of Skinker and White⁵² to calculate the dashed ν_m/N and ν_u/N curves of Fig. 9. We have not, however, tried to obtain cross sections corresponding to the range of ϵ_K , i.e., $\epsilon_K > 0.6$ eV, for which no w data are available. This means that we will determine cross sections only for electron energies below about 1 eV. At higher electron energies, we will use the elastic⁵⁵ and inelastic⁵⁶ cross sections given by others. The cross sections derived from our analysis are shown in Figs. 10 and 11 and the values of the transport coefficients calculated using these cross sections are shown by the solid lines of Fig. 8 and the points of Fig. 9.

The ν_u/N curve of Fig. 9 suggests that the dominant energy-loss processes change at ϵ_K near 0.08 and 0.7 eV. Our analysis shows that (a) rotational excitation and de-excitation are of primary importance from thermal energies ($kT = 0.00663$ eV) to about 0.06 eV, (b) "direct" vibrational excitation dominates between 0.1 and 0.6 eV, and (c) resonant vibrational excitation and electronic excitation dominate for $\epsilon_K > 0.8$ eV. We are primarily concerned with the first two of these processes.

A. Rotational Excitation ($\epsilon_K < 0.06$ eV, $E/N < 5 \times 10^{-18}$ V cm²)

Our analysis of the rotational excitation process in CO consists of finding the effective dipole moment which is required to make the formulas for the effect of rotational excitation give a good fit to the experimental ν_u/N data. This procedure is similar to that adopted previously¹⁻³ for H₂ and N₂ and is necessary because of the large number of rotational levels which are thermally excited even at 77°K. According to Takayanagi,⁴⁷ the cross section for rotational excitation is given by

$$\sigma_{J,J+1}(\epsilon) = \frac{(J+1)R_y\sigma_r}{(2J+1)\epsilon} \ln \frac{[\epsilon^{1/2} + (\epsilon - \epsilon_J)^{1/2}]}{[\epsilon^{1/2} - (\epsilon - \epsilon_J)^{1/2}]}, \quad (5)$$

where $\sigma_r = 8\pi\mu^2 a_0^3/3$, μ is the electric dipole moment in units of ea_0 , a_0 is the Bohr radius, J is the rotational quantum number of the initial state, and R_y is the Rydberg (13.6 eV). The threshold energy and the

⁵⁴ Since it can be shown that the magnetic drift velocity w_M is always larger than or equal to the time-of-flight drift velocity, the ν_m/N and ν_u/N values calculated using the magnetic drift velocity will be smaller and larger, respectively, than the values calculated using w . For CO the calculations using our derived cross sections give $w_M/w \approx 1.5$ for $\epsilon_K = 0.07$ eV and lower values at higher and lower ϵ_K . One reason for distrusting the w_M data in CO is that negative-ion formation and associative detachment were not taken into account in the analysis of the experiments. See J. L. Moruzzi and A. V. Phelps, *J. Chem. Phys.* **45**, 4617 (1966).

⁵⁵ C. Ramsauer and R. Kollath, *Ann. Physik* **10**, 143 (1931); R. Kollath, *ibid.* **15**, 485 (1932). The present authors thank K. Takayanagi for the copies of his unpublished evaluation of momentum transfer cross sections obtained by analysis of beam experiments which led to these considerations. It is to be noted that maximum in the total cross section given by Ramsauer and Kollath in Ref. 34 occurs at significantly lower energies than that given by Brode in Ref. 42.

⁵⁶ G. J. Schulz, *Phys. Rev.* **116**, 1141 (1959); and Ref. 25.

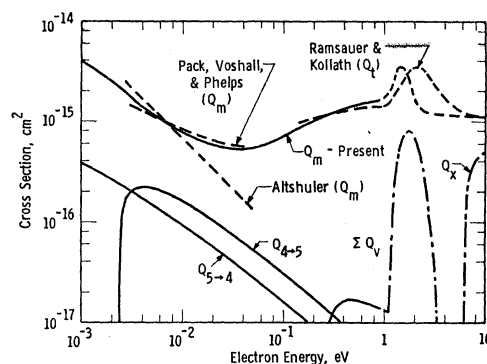


Fig. 10. Momentum-transfer and inelastic-scattering cross sections for electrons in CO. The solid lines show the cross sections derived from our analysis of the data of Figs. 8 and 9. For simplicity we have shown only two of the many rotational excitation and de-excitation cross sections and have shown only the sum of the vibrational excitation cross sections ΣQ_v . Note that the rotational excitation cross sections shown include a factor equal to a fraction of the molecules in the initial rotational level at 77°K.

energy lost by an electron is $\epsilon_J = 2(J+1)B_0$, where B_0 is the rotational constant for the molecule.⁵⁷ For CO, $B_0 = 2.4 \times 10^{-4}$ eV, so that a typical threshold ($J=4$) occurs at 2.4×10^{-3} eV. The cross section for de-excitation of the J th rotational level is given by

$$\sigma_{J,J-1}(\epsilon) = \frac{JR_y\sigma_r}{(2J+1)\epsilon} \ln \frac{[(\epsilon + \epsilon_J)^{1/2} + \epsilon^{1/2}]}{[(\epsilon + \epsilon_J)^{1/2} - \epsilon^{1/2}]}. \quad (6)$$

Here $\epsilon_J = 2JB_0$ is the energy gained by the electron. As

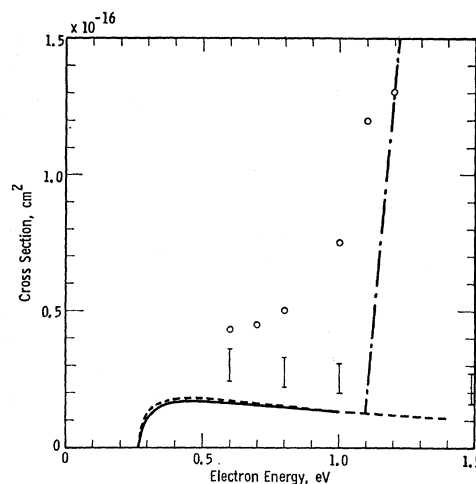


Fig. 11. Low-energy portion of the cross section for excitation of the first vibrational state of CO. The solid curve shows the cross section which we obtain by analysis of the data of Figs. 8 and 9. The nearly vertical line above 1.1 eV is an interpolation between our derived cross section and the cross section given by Schulz (open circles). The transition was taken at 1.1 eV because Schulz's data show a very rapid increase in cross section starting at this energy. The vertical bars show the results of the theory of Breig and Lin. The short dashed curve is the cross section obtained using the theory given by Takayanagi.

⁵⁷ G. Herzberg, *Spectra of Diatomic Molecules* (D. Van Nostrand Company, Inc., Princeton, New Jersey, 1950), p. 521.

in previous papers,¹⁻³ we are concerned with an effective cross section Q which is equal to the cross sections given in Eqs. (5) and (6) multiplied by the fraction of the molecules in a particular rotational state. Thus,

$$Q_{J,J+1} = (p_J \sigma_{J,J+1} / P_r) \exp[-J(J+1)B_0/kT],$$

where

$$P_r = \sum_J p_J \exp[-J(J+1)B_0/kT]$$

and $p_J = (2J+1)$. Typical rotational excitation and de-excitation cross sections, i.e., $Q_{4,5}$ and $Q_{5,4}$, are shown in Fig. 10 for CO at 77°K. These curves were calculated using our effective dipole moment of $4.6 \times 10^{-2} ea_0$.

As is the case for all gases except H₂ and D₂, the thresholds for rotational excitation in CO are so small compared to kT that we have been able to solve the Boltzmann equation using the exact set of rotational excitation and de-excitation cross sections only for a small range of ϵ_K at low kT , e.g., $\epsilon_K < 3kT$ at 77°K. For $\epsilon_K > 3kT$ we have used a modification of the continuous approximation to rotational excitation developed originally¹ for gases in which rotational transitions occur as a result of the electric quadrupole moment. Thus, the substitution of Eqs. (5) and (6) into Eq. (8) of Ref. 1 and the subsequent expansion for $\epsilon \gg kT$ yields⁵⁸ an expression for the net contribution of rotational excitation to the Boltzmann equation Z , which is

$$\frac{Z}{N} = 2B_0 \sigma_r R_y \frac{d}{d\epsilon} \left[f(\epsilon) \ln \frac{2\epsilon}{(B_0 kT)^{1/2}} \right], \quad (7)$$

where $f(\epsilon)$ is the electron-energy distribution function.

When Eq. (7) is used in the Boltzmann equation in place of Eqs. (5) and (6) for $0.02 < \epsilon_K < 0.06$ eV and when we use an effective dipole moment of $4.6 \times 10^{-2} ea_0$, we obtain the solid points of Fig. 9. Figure 9 also shows

⁵⁸ Because of the logarithmic energy dependence of Eqs. (5) and (6) for $\epsilon \gg 2JB_0$, the derivation of Eq. (7) is not as straightforward as is the corresponding derivation for molecules in which rotational excitation occurs via a quadrupole transition (Ref. 1). This is particularly noticeable when one compares the continuous approximation with the high-energy limit of the single-level approximation as in the Appendix. Somewhat less difficulty is encountered when the logarithmic terms in Eqs. (5) and (6) are approximated by $2(\epsilon/\epsilon_J)^{-1/4}[(\epsilon/\epsilon_J) - 1]^{1/2}$ and $2(1 + \epsilon/\epsilon_J)^{-1/4}(\epsilon/\epsilon_J)^{1/2}$, respectively. The approximation for Eq. (5) yields cross sections which are exact for $\epsilon \rightarrow \epsilon_J$, approximately less than 8% low for $\epsilon = 2\epsilon_J$, and less than 5% too large for $\epsilon = 150\epsilon_J$. Similarly, for Eq. (6). The approximations are therefore useful over the range of electron energies of interest to us. With this approximation, Eq. (7) becomes

$$Z/N = \Gamma(15/8) R_y \sigma_r (2)^{7/8} (B_0)^{7/8} (kT)^{-1/8} \frac{d}{d\epsilon} [e^{1/4} f(\epsilon)],$$

and the cross section for excitation in the single-level approximation is

$$Q_0 = \Gamma(15/8) \sigma_r [1 - \exp(-2B'/kT)]^{-1} (R_y/B') (B_0/B')^{3/4} \times (B_0/kT)^{1/8} (2B'/\epsilon)^{5/4} [(\epsilon/2B') - 1]^{1/2}.$$

These approximations had not been worked out at the time of the numerical calculations discussed in this paper but have been used in a recent analysis of NO data and agree with earlier CO results. A similar power-law approximation to the Born-approximation result has been used by A. E. S. Green and C. A. Barth, J. Geophys. Res. **70**, 1083 (1965).

the results at calculations in the near thermal region, $\epsilon_K < 0.02$ eV, using (a) 16 rotational levels and the "exact" solution of Ref. 1 and (b) an extrapolation of the continuous approximation to low ϵ_K including thermalization effects.¹ The ν_u/N and ν_m/N values calculated using the 16 rotational levels with $\mu = 4.6 \times 10^{-2} ea_0$ are shown by the open points in Fig. 9. These ν_u/N values are only slightly smaller than those calculated using the continuous approximation, i.e., Eq. (7), and shown by solid points. The single-level approximation discussed in the Appendix gave a similar result for reasonable threshold energies. In fact a threshold energy for the single-level approximation of $3kT$ was required in order to approximate the rising ν_u/N curve for ϵ_K below 0.01 eV. This suggests that the experimental ϵ_K values for CO are too high at low E/N and that, as in the case of elastic collisions only,⁵⁹ a decrease in ν_u/N as ϵ_K approaches kT is not to be expected in CO where there is little variation of the momentum transfer collision frequency with electron energy near $\epsilon = kT$.

The magnitude of the effective dipole moment for CO derived from the preceding analysis is $4.6 \pm 0.5 \times 10^{-2} ea_0$ as compared to a Stark-shift value⁶⁰ of $4.4 \times 10^{-2} ea_0$. This difference is well within the accuracy of our determination. More accurate theoretical calculations of the rotational excitation cross sections would be very desirable,⁴⁷ although refined calculations^{37, 61} for rotational excitation of N₂ via the quadrupole moment have resulted in only a small decrease in the cross section in the energy range of interest here.

It should be noted that the difference between the smooth curve and the calculated points for ν_u/N near 0.07 eV in Fig. 9 can very probably be accounted for by our omission of rotational excitation via the electric quadrupole moment. Thus, the quadrupole moment and rotational constant for CO are very close to those for N₂ so that the contribution to ν_u/N should be nearly the

⁵⁹ We have investigated the near thermal region for gases with elastic collisions only using a perturbation approach. It is found that as

$$\epsilon_K \rightarrow kT, \quad \nu_u/\nu_m = (3m/M) [\Gamma(5/2 - n/2)]^2 \times [\Gamma(5/2 - 3n/2) \Gamma(5/2)]^{-1} \leq (3m/M),$$

where we have assumed that the frequency of momentum transfer collisions varies as $\epsilon^{n/2}$ and $n < 2$. On the other hand, for

$$\epsilon_K \gg kT, \quad \nu_u/\nu_m = (3m/M) [\Gamma(5/2 - 4s)]^2 \times [\Gamma(5/2 - 3s)]^{-2} [\Gamma(5/2 - 6s)]^{-1},$$

where $s = n(2n+2)^{-1}$ and $n > -1$. These results are in good agreement with experimental data for $\epsilon_K \rightarrow kT$ at 300°K in He ($n \sim 1.4$) and argon ($n \sim 0.25$). These arguments suggest that one should not expect a decrease in ν_u/N as $\epsilon_K \rightarrow kT$ in CO since the electron collision frequency is nearly constant for $\epsilon \sim kT$ but one should expect the large decrease observed in N₂, where $n \sim 1$. We are indebted to P. G. Klemens for helpful discussion of the perturbation solution. We have not been able to obtain useful analytical solutions for one or more discrete energy-loss processes.

⁶⁰ C. A. Burrus, J. Chem. Phys. **28**, 427 (1958).
⁶¹ R. C. Mjolsness and D. H. Sampson, Phys. Rev. Letters **13**, 812 (1964); K. Takayanagi and S. Geltman, Phys. Rev. **138**, A1003 (1965); D. H. Sampson and R. C. Mjolsness, *ibid.* **140**, A1466 (1965).

same as for N_2 , i.e., 1.0×10^{-11} cm²/sec for CO at $\epsilon_K = 0.07$ eV.

B. "Direct" Vibrational Excitation ($0.1 < \epsilon_K < 0.6$ eV)

Cross section for vibrational excitation of CO by a "direct" or "nonresonant" process have been calculated by Wu⁴⁷, by Takaganagi,⁴⁷ and by Breig and Lin.⁴⁹ Using the Born approximation, the cross section for vibrational excitation is given by

$$Q_{BV} = \sigma_v \frac{R_y}{\epsilon} \ln \frac{[\epsilon^{1/2} + (\epsilon - \epsilon_v)^{1/2}]}{[\epsilon^{1/2} - (\epsilon - \epsilon_v)^{1/2}]}, \quad (8)$$

where $\sigma_v = 8\pi |\langle v' | \mu | v \rangle|^2 a_0^2 / 3$, and ϵ_v is the separation of the v' and v vibrational levels. We are concerned only with the $v=0, v'=1$ transition, since the cross sections for direct excitation of the higher levels are expected to be small^{47,62} and since only the $v=0$ level is significantly populated. Using⁶² $\epsilon_v = 0.266$ eV and $|\langle 1 | \mu | 0 \rangle|^2 = 1.66 \times 10^{-3}$ in units of $e^2 a_0^2$, we obtain the cross section for the excitation of the first vibrational state of CO as shown by the dashed curve of Fig. 11. The solid curve of Fig. 11 shows cross section which we found necessary to give a good fit to the ν_u/N data for $0.1 < \epsilon_K < 0.6$. The ν_u/N values obtained using this cross section are shown by the points in Fig. 9 for $0.09 < \epsilon_K < 0.7$ eV. We conclude that the cross sections determined by our analysis are in very good agreement with the simple dipolar theory of vibrational excitation for electron energies below 1 eV. We note that the vibrational excitation cross section given by Eq. (8) and derived by our analysis at say 0.5 eV is approximately 30 times the vibrational excitation cross section for N_2 at the same energy.³ This difference is presumably due to the effect of the dipole moment of the CO molecule and suggests that the interactions which determine the low-energy vibrational excitation cross section⁴⁹ in N_2 are not important in CO.

Figure 11 also shows the cross sections for excitation of the first vibrational level as calculated by Breig and Lin⁴⁹ including polarization effects using the Born approximation. The results of this calculation are significantly larger than the values which we derive from experiment. The poorer agreement found here may possibly be related to the poorer agreement found³ when a polarization term is added to the quadrupole potential and the cross sections for rotational excitation of N_2 are calculated using the Born approximation.⁶¹ Furthermore, one notes that vibrational cross section calculated using no polarization correction for electrons near threshold in N_2 gives very good agreement with experiment.³ Thus, our analysis of rotational and vibrational excitation near threshold in CO and N_2 suggests that the

addition of polarization effects worsen the Born-approximation result for these problems.

The cross sections for excitation of the first vibrational level of CO as determined by Schulz²⁴ from electron scattering at 72° are shown by the circles in Fig. 11. The large disagreement at the lower energies is believed to be well outside the experimental errors and is therefore attributed to departure from isotropic scattering. Further studies of this point are desirable.

As indicated previously, the inelastic cross sections used in our analysis for electron energies above 1 eV are not adjusted to fit the experimental transport-coefficient data. These cross sections are included in order to insure a reasonable behavior of the electron-energy distribution function at energies above 1 eV. The electron-energy distribution functions calculated for CO resemble those calculated³ for N_2 in that the distribution function drops rapidly at electron energies for which the vibrational excitation cross section is large. This behavior enhances the separation of the effects of the threshold and resonant regions of the vibrational excitation cross sections. The cross sections used, and shown in Fig. 10, are the vibrational excitation cross sections given by Schulz and an electronic excitation cross section with a threshold at 6 eV as suggested by electron-beam data,^{24,40} but of arbitrary magnitude.⁶³ The fact that the ν_u/N values calculated using these cross sections lie above the curve calculated using experimental w_M values suggests that the vibrational excitation cross sections for energies above 1 eV are too large. Obviously, further investigation for $\epsilon_K > 0.7$ eV is desirable.

C. Momentum-Transfer Cross Section

The momentum-transfer cross section for electrons in CO as determined from our analysis for energies below about 1 eV is shown by the upper solid curve of Fig. 10. As shown previously,⁵⁰ the Q_m curve for CO is approximately given by the sum of a dipole term, such as calculated by Altshuler⁴⁶ and a nitrogenlike cross section. The short dashed curve in Fig. 10 marked "Altshuler" is calculated using our derived dipole moment of $4.6 \times 10^{-2} ea_0$. The theory of Mittelmann and von Holt⁴⁸ gives the same result for a molecule with as small a dipole moment as that of CO. It should be kept in mind that the value of Q_m given by these theories is essentially the sum of the rotational excitation cross sections appropriately weighted over scattering angle and neglecting energy loss by the electrons. Accordingly, we can test the theory only for ϵ_K significantly larger than kT . Also, in the near thermal range there may be some question as to the validity of the solution of the Boltzmann equation which we are using, since this

⁶² S. S. Penner, *Quantitative Molecular Spectroscopy and Gas Emissivities* (Addison-Wesley Publishing Company, Inc., Reading, Massachusetts, 1959), p. 23. According to this reference, $|\langle 2 | \mu | 0 \rangle|^2 / |\langle 1 | \mu | 0 \rangle|^2 = 3.5 \times 10^{-3}$ for CO.

⁶³ This process has the lowest excitation threshold of any electronic process (Ref. 57) in CO and was included in our calculations in order to prevent electrons which penetrate the vibrational barrier from reaching unrealistically large energies. The magnitude chosen for this cross section is probably much larger than true excitation cross section for this state.

solution is based on the assumption that the inelastic-scattering cross sections are small compared to the elastic-scattering cross section.² Further investigations of these points are desirable.

The momentum-transfer cross section used in our calculations for $\epsilon_K > 0.7$ eV and electron energies above 1 eV is shown by the upper short and long dashed line of Fig. 10. It was chosen to extrapolate smoothly to our derived curve at lower energies and peaks at an energy somewhat below that of total cross section³³ as required by the angular scattering data of Ramsauer and Kollath.⁵⁵ The magnitude of the peak is larger than indicated by the electron-beam data,^{33,40} but judging from the comparison of the experimental curves and the points, one should raise Q_m values at electron energies above 1 eV even further. We believe that such an analysis should await better experimental data in the high- ϵ_K range.

IV. CARBON DIOXIDE

An analysis of electron transport coefficient data in CO_2 was undertaken because of the very large energy exchange frequency at very low ϵ_K and the availability of recent time-of-flight drift velocity and ϵ_K data. More recently, the interest in excitation cross sections for electrons in CO_2 has increased because of the development of CO_2 lasers. The experimental drift velocity and ϵ_K data^{9,50,51,64-71} for electrons in CO_2 are shown by the points in Fig. 12. Smooth curves through these points (not shown) were used to calculate the ν_m/N and ν_u/N curves of Fig. 13. Note that because of the absence of drift velocity data for $2.5 \times 10^{-16} < E/N < 1 \times 10^{-15}$ Vcm², we cannot calculate ν_m/N and ν_u/N for $0.6 < \epsilon_K < 3$ eV. In addition to adjusting our cross sections so as to obtain a fit between the experimental and calculated values of ν_m/N and ν_u/N , we have adjusted the cross sections so as to yield a fit of experimental and calculated values of the net ionization coefficients^{72,73} $(\alpha_i - \alpha_a)/N$ as shown in Fig. 14. Figure 14 also shows experimental and calculated attachment coefficients.⁷²⁻⁷⁴ The cross sections which we have derived from the experimental data are shown in Figs. 15 and 16.

The threshold for excitation of the lowest vibrational

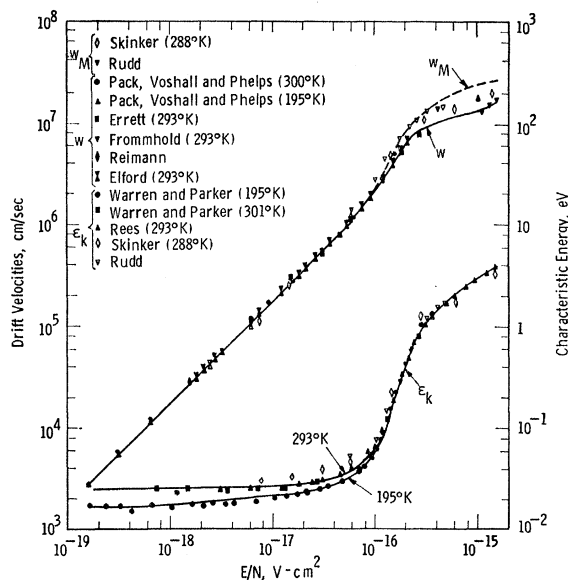


FIG. 12. Drift velocities and characteristic energy of electrons in CO_2 . The experimental results are shown by points and the results of our calculations using the cross sections of Fig. 14 are shown by smooth curves. Some experimental data are omitted for the sake of clarity.

state of CO_2 is so low in energy, 0.083 eV, and the sublimation temperature for CO_2 at atmospheric pressure is so high, i.e., $kT_s = 0.0168$ eV, that we are unable to obtain data in which ν_u/N is clearly determined by rotational excitation. The ν_u/N values due to rotational

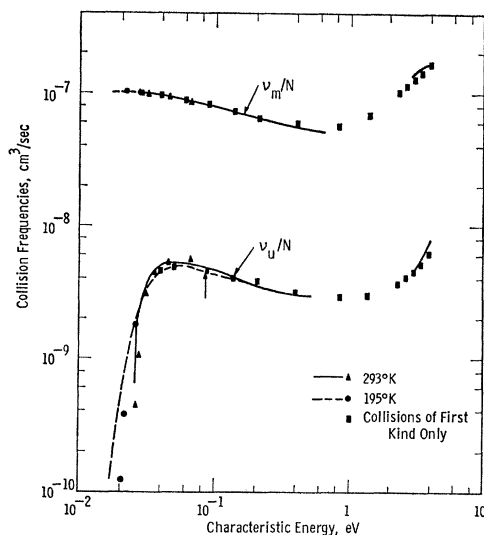


FIG. 13. Momentum-transfer and energy-exchange collision frequencies per molecule for electrons in CO_2 . The smooth curves are calculated from smooth curves through selected w and ϵ_K data plotted in Fig. 12. The points show the results of calculations using the cross sections of Figs. 15 and 16. The arrow indicates a characteristic energy equal to the threshold for excitation of the lowest vibrational state, i.e., $\epsilon_K = 0.083$ eV.

⁶⁴ M. F. Skinker, *Phil. Mag.* **44**, 994 (1922).

⁶⁵ J. B. Rudd, as given in Ref. 8.

⁶⁶ D. Erret, Ph.D. thesis, Purdue University, 1951 (unpublished).

⁶⁷ T. E. Bortner, G. S. Hurst, and W. G. Stone, *Rev. Sci. Instr.* **28**, 103 (1957); N. E. Levine and M. A. Uman, *J. Appl. Phys.* **35**, 2618 (1964).

⁶⁸ L. Frommhold, *Z. Physik* **160**, 554 (1960).

⁶⁹ L. W. Cochran and D. W. Forester, *Phys. Rev.* **126**, 1785 (1962).

⁷⁰ J. A. Rees, *Australian J. Phys.* **17**, 462 (1964).

⁷¹ M. T. Elford, *Australian J. Phys.* **19**, 629 (1966).

⁷² M. S. Bhalla and J. D. Craggs, *Proc. Phys. Soc. (London)* **76**, 369 (1960).

⁷³ H. Schlumbohm, *Z. Physik* **166**, 192 (1962).

⁷⁴ P. A. Chatterton, *Proc. Phys. Soc. (London)* **85**, 355 (1965).

excitation as calculated²⁶ using a quadrupole moment⁷⁵ of $3ea_0^2$ and $B_0=4.85\times 10^{-5}$ eV⁷⁶ are expected to be roughly equal to that for N_2 , i.e., about 1.7×10^{-11} cm²/sec at $\epsilon_K=0.04$ eV. Since the values of ν_u/N shown in Fig. 13 are much larger than this, we neglect rotational excitation in our analysis and assume that the observed energy losses are due to vibrational and electronic excitation only.⁷⁷ The ν_u/N data of Fig. 13 are consistent with a change in the dominant energy-loss process near $\epsilon_K=1$ eV and we divide our discussion of the analysis into regions below and above this ϵ_K value.

A. Low-Energy Region ($\epsilon_K < 1$ eV, $E/N < 3\times 10^{-16}$ V cm²)

Our determination of the low-energy excitation cross sections is based on the assumption that the cross

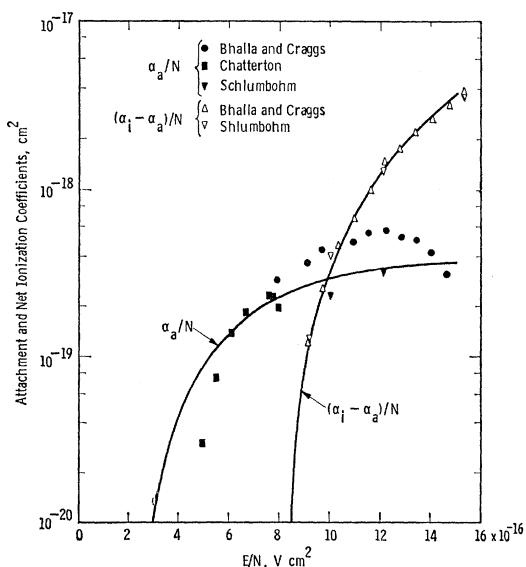


FIG. 14. Attachment and net ionization coefficients for electrons in CO₂. The points show the experimental values and the curves show the results of our calculations using the cross sections of Fig. 16 and the attachment cross section of Schulz.

sections are those for vibrational excitation. The cross sections are assumed to include components due to the same transitions as those observed in infrared absorption⁶² as well as the resonance structure found by Schulz⁷⁸ from the inelastic scattering of electrons through an angle of 72°. The derived cross sections are shown in Figs. 15 and 16. The resonance nature of the

⁷⁵ R. H. Orcutt, J. Chem. Phys. **39**, 605 (1963); A. A. Maryott and S. J. Kryder, *ibid.* **41**, 1580 (1964).

⁷⁶ G. Herzberg, *Molecular Spectra and Molecular Structure* (D. Van Nostrand Company, Inc., Princeton, New Jersey, 1960), Vol. II.

⁷⁷ At ϵ_K values below 0.025 eV our calculated ν_u/N values are too low. We do not know whether this is due to measured values of ϵ_K which are systematically too low at low E/N or whether the rotational excitation cross sections are significantly larger than given by the quadrupole formulas of Ref. 26.

⁷⁸ G. J. Schulz (unpublished).

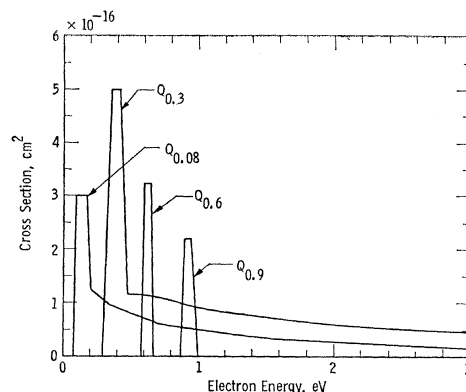


FIG. 15. Cross sections for vibrational excitation of CO₂ by electron impact. The subscripts to the Q 's are the approximate energy losses assigned to the various cross sections.

cross sections with energy losses and thresholds at 0.3, 0.6, and 0.9 eV and the high energy tail of the 0.3-eV process were observed by Schulz.⁷⁸ The magnitudes of these cross sections, the magnitudes of the resonance portion of the 0.083-eV energy-loss process, and the $Q_m(\epsilon)$ curve were adjusted to give a good fit to ν_m/N and ν_u/N curves calculated from the 293°K data of Rees⁷⁰ and of Elford⁷¹ and to the 195°K data. One notes that the portion of the ν_u/N curves for $\epsilon_K < 0.05$ eV requires a very large cross section near the threshold for the lowest energy vibrational state, i.e., the 01⁰ level at 0.083 eV.

The energy dependences of the nonresonance or direct excitation portions of the cross sections for the 0.083 and 0.3 eV energy-loss process are calculated using Eq. (8) and transition probabilities of 4×10^{-8} and $1.2\times 10^{-2}e^2a_0^2$, respectively. Since direct excitation of the 0.083-eV level makes only a small contribution to ν_u/N in the critical energy range near $\epsilon_K=0.4$ eV, the effective transition probability is assumed to be equal to the value obtained from infrared-absorption experiments.⁶² It was necessary to assume an effective transi-

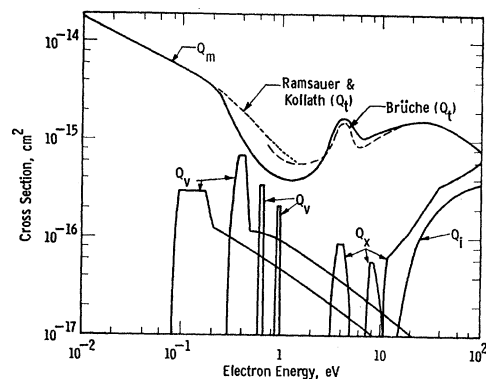


FIG. 16. Cross sections for momentum transfer and inelastic scattering of electrons in CO₂. The solid curves show the cross sections derived in our analyses of the data of Fig. 13. The broken curves labeled Q_t give the results of electron-beam measurements of the total electron-scattering cross section. The cross section for dissociative attachment is too small to appear on this plot.

tion probability for the excitation of the 00⁰1 level equal to 75% of the value obtained from infrared data⁶² in order to fit the ν_u/N curve over the whole range of ϵ_K . The contribution to the energy loss calculated using Eq. (8) and the measured infrared transition probabilities⁶² for higher vibrational levels is negligible. Approximate agreement with the Born approximation cross sections for the 01⁰ and 00⁰1 levels has been obtained at 33 keV by Geiger and Wittmaack.⁷⁹ Note that we have effectively associated all of the observed 0.3-eV energy loss with excitation of the 00⁰1 level. It is tempting to ascribe the 0.6 and 0.9 eV resonances to excitation of the 00⁰2 and 00⁰3 levels. Also, we note that if we omit the resonance portions of the cross sections and use the measured infrared transition probabilities, we can obtain good agreement with ν_u/N data for ϵ_K near 0.4 eV, but that the calculated ν_u/N values are low by approximately a factor of 2 at $\epsilon_K \sim 0.04$ eV. In a preliminary analysis,⁸⁰ we were able to obtain reasonable agreement with experiments while essentially neglecting the contribution of direct excitation, i.e., using resonance peaks as above but with very small Q_{vib} at higher energies. The high-energy tails were added because Schulz observed such behavior and because of the good agreement between theory and experiment found in Sec. III for the vibrational excitation of CO.

The low-energy portion of the derived cross section for excitation of the 0.083-eV level is very accurately determined ($\pm 10\%$) by our curve-fitting process once the general shape of the cross section is fixed. We have not attempted to fit a typical "resonance" curve⁸¹ to the ν_u/N data. The cross sections derived for the higher-energy resonances are probably best described in terms of the integral of the cross section over the resonance region, i.e., 5×10^{-17} , 2×10^{-17} , and 2×10^{-17} cm² eV for the 0.3, 0.6, and 0.9 eV resonances, respectively.

At very low energies the derived Q_m curve varies as $\epsilon^{-1/2}$, i.e., the electron collision frequency per molecule is constant. This result is consistent with the temperature independence of the thermal electron mobility found previously.⁵⁰ Some direct evidence for the deep minimum in $Q_m(\epsilon)$ is noted in the angular-scattering data⁵⁵ for electrons in CO₂. These data show a pronounced peak of scattered electrons in the forward direction as the electron energy is reduced toward 1 eV. The deep minimum in $Q_m(\epsilon)$ and the large resonance peaks in the vibrational excitation cross sections between 0.3 and 1 eV lead to relatively poor separation of elastic and inelastic effects using our ν_m/N and ν_u/N variables at ϵ_K values between 0.2 and 1.0 eV. In this connection, one should investigate the possibility that

the fact that $\nu_u \ll \nu_m$ is not a sufficient condition for the validity⁸² of the present calculations when the ratio of the inelastic to elastic cross sections is not small compared to unity.

B. Moderate-Energy Region ($\epsilon_K > 1.0$ eV, $E/N > 3 \times 10^{-16}$ V cm²)

The choice of the excitation processes to be used to fit the ν_u/N and $(\alpha_i - \alpha_a)/N$ data is based largely on the "trapped electron" data of Schulz^{25,40,78} which shows prominent peaks in the energy-loss spectrum with apparent thresholds at 3.1, 7.0, and 10.5 eV. The effects of other excitation processes are included in these effective cross sections. As usual, our analysis determines the rising portions of the cross sections most accurately. The relative magnitudes and the energy dependences of the 3.1- and 7.0-eV cross sections were kept fixed at the values suggested by Schulz's threshold data. The absolute values were then determined primarily by fitting the calculated points to the experimental ν_u/N curve of Fig. 13 for $0.8 < \epsilon_K < 2$ eV. We note that if an inelastic process for which we have assumed the energy loss to be the threshold energy is actually an approximation to a large number of vibrational excitation processes, then the energy losses will be smaller than we have assumed and the sum of the vibrational cross sections will be significantly larger than assumed. This may well be the case for our 3.1-eV energy loss process. Electron-beam data such as those of Schulz²⁵ for N₂ and CO would be required in order to carry out a significantly more accurate analysis than that given here.

The determination of inelastic cross sections in the $\epsilon_K > 1.0$ eV range was made more accurate by the use of the measured attachment⁴⁰ and ionization⁸³ cross sections and the measured net ionization coefficients^{72,73} $(\alpha_i - \alpha_a)/N$. As in O₂, we chose to fit to the $(\alpha_i - \alpha_a)/N$ data because it appears that this quantity is more accurately measured than either α_i/N or α_a/N . Thus, the shape and magnitude of the 10.5-eV excitation cross section and, to some extent, the magnitudes 3.1- and 7.0-eV processes were adjusted to yield the fit of the calculated and experimental values of ν_u/N ($\epsilon_K > 2$ eV) and $(\alpha_i - \alpha_a)/N$ values shown in Figs. 13 and 14. Figure 14 also shows a comparison of calculated and measured attachment coefficients α_a/N . For $E/N > 6 \times 10^{-16}$ V cm², the calculated α_a/N values are within the rather large spread of the experimental values. As the E/N value is decreased below 6×10^{-16} V cm², the ratio of calculated to experimental α_a/N values increases in a manner similar to that found in Sec. II for O₂. We have no explanation for this discrepancy, although it may be related to the unexplained low threshold for negative ion

⁷⁹ J. Geiger and K. Wittmaack, Z. Physik **187**, 433 (1965).

⁸⁰ R. D. Hake, Jr., and A. V. Phelps, Bull. Am. Phys. Soc. **12**, 232 (1967).

⁸¹ E. Baranger and E. Gerjuoy, Proc. Phys. Soc. (London) **72**, 366 (1958); A. Herzenberg and F. Mandl, Proc. Roy. Soc. (London) **A270**, 48 (1962); J. C. Y. Chen, J. Chem. Phys. **45**, 2710 (1966); and Ref. 49.

⁸² T. Holstein, Phys. Rev. **70**, 367 (1946); S. Althuler, J. Geophys. Res. **68**, 4707 (1963); G. A. Baraff and S. J. Buchsbaum, Phys. Rev. **130**, 1007 (1963).

⁸³ D. Rapp and P. Englander-Golden, J. Chem. Phys. **43**, 1464 (1964).

formation found with electron beam techniques.^{40,84} We were unable to significantly improve the fit of the calculated and measured values of α_a/N by assigning a small energy loss to a resonance occurring near the threshold for attachment as was done for O₂ in Sec. II B.

The momentum-transfer cross section derived for $\epsilon > 2$ eV by fitting the ν_m/N curves and shown by the solid curve in Fig. 16 is similar to the total cross section Q_t found by electron-beam techniques and shown by the dashed curve. A striking feature of these curves is the peak at about 4 eV. The relatively narrow width of this peak and its coincidence with a maximum in the energy-loss spectrum observed by Schulz⁷⁸ suggests that this structure is due to a resonance of the type found²⁵ in N₂, CO, etc. This suggestion is supported by the fine structure in the elastic-scattering cross section found by Boness and Hasted.²⁴ The occurrence of the peak of the attachment cross section at an energy⁴⁰ (4.4 eV) higher than that of the maximum in the elastic and inelastic cross section is expected because the threshold for dissociative attachment (3.9 eV) occurs near the peak of the resonance at 4.0 eV. The model just described is somewhat similar to that proposed by Schulz and Asundi⁸⁵ for the dissociative attachment process in H₂ at energies near 3.7 eV.

Finally, it is of interest to note that although our procedure of fitting to the ν_m/N and ν_u/N curves leads to rather satisfactory agreement between the calculated and experimental w and ϵ_K values shown in Fig. 12, the agreement between calculated and experimental values of w_M for $E/N > 3 \times 10^{-16}$ V cm² is poor. It is claimed⁶⁴ that the effect of negative ion formation was small under the conditions of Skinker's measurements. Further experimental and theoretical investigations of this E/N range are necessary in order to resolve this discrepancy.

V. DISCUSSION

The analyses of electron-transport coefficients in terms of elastic and inelastic cross sections presented above show that many interesting conclusions can be reached regarding the magnitude and energy dependence of the cross sections. Because of the poor fractional energy resolution characteristics of equilibrium electron-energy distributions, i.e., a half-width roughly equal to the mean energy, our analyses have been made considerably more unique by the use of the available energy dependence of the excitation cross sections obtained from electron-beam experiments. However, even with this additional information we are left with a lack of uniqueness in the final cross sections, e.g., the details of the vibrational excitation cross sections in O₂. Fortunately there are cases, such as the vibrational excitation of CO and of CO₂ near threshold, in which we are

confident of a high degree of accuracy ($\pm 10\%$) in the derived cross section in spite of our inability to prove uniqueness. We expect the derived values of $Q_m(\epsilon)$ to be accurate to $\pm 10\%$ for CO at $\epsilon < 1$ eV and for CO₂ at $\epsilon < 0.2$ eV and accurate to $\pm 30\%$ for O₂ at $0.1 < \epsilon < 8$ eV and for CO₂ at $0.2 < \epsilon < 15$ eV. Even with these qualifications, we believe that the desired cross sections give a good description of the processes involved and will allow a reasonably accurate calculation, $\pm 10\%$ in most cases, of transport coefficients, total excitation rates, etc., in O₂, CO, and CO₂ and in mixtures of these gases with other gases for which cross sections are available, i.e., N₂, H₂, and the rare gases.

The electron-scattering cross sections for N₂, O₂, and CO₂ are of particular significance with regard to the prediction of the properties of low-energy electrons in air. Nitrogen has been analyzed previously.³ Carbon dioxide was considered in Sec. IV. As indicated in Sec. II, there is still considerable uncertainty regarding the cross sections for momentum-transfer collisions and rotational excitation by electrons in O₂ at electron energies below about 0.2 eV. Until these cross sections are agreed upon there will remain an uncertainty in the ν_m/N and ν_u/N values for thermal electrons in dry air of approximately 10% and up to a factor of 1.8, respectively. As pointed out in Sec. II C, the vibrational excitation of O₂ is the dominant energy-loss process for electrons in air for electron energies between 0.2 and 1.7 eV.

Our final comment is a plea for additional high-quality experimental electron transport-coefficient data so as to fill in the many gaps and check the questionable data evident for the various gases and gas temperatures discussed in this paper. Once such data are available for gases such as CO₂, H₂O, and CH₄ over a wide range of E/N values it will be necessary to examine carefully the procedures used for the calculation of electron-energy distribution functions and transport coefficients in these gases, i.e., for gases in which the inelastic cross sections are comparable with the elastic-scattering cross sections.

Tabulations of cross sections and calculated transport coefficients are available on request.⁸⁶

ACKNOWLEDGMENTS

The authors wish to express their appreciation for valuable discussions of this work with their associates in the Atomic Physics Group, particularly G. J. Schulz. We also wish to thank A. G. Engelhardt, D. P. Wei, and E. Geil for assistance in adapting the computer programs to the present problems.

APPENDIX A: SINGLE-LEVEL APPROXIMATION

The purpose of this Appendix is to derive the relations appropriate to the single-level approximation for the calculation of the effects of rotational excitation. This

⁸⁴ P. J. Chantry and G. J. Schulz, Phys. Rev. Letters **12**, 449 (1964); Phys. Rev. **156**, 134 (1967).

⁸⁵ G. J. Schulz and R. K. Asundi, Phys. Rev. Letters **15**, 946 (1965).

⁸⁶ See Appendix of Westinghouse Scientific Paper 66-1E2-GASES-P1 (unpublished).

approximation was used at low ϵ_K for O_2 in Sec. II and the results of such calculation for CO were discussed in Sec. III. The reasons for considering such an approximation are (a) the large amount of computer time required for the exact solution using many rotational levels; (b) our inability to use the exact solution with a program written for an IBM 7094 computer when $\epsilon_K > 40B_0$ for rotational excitation via a quadrupole transition^{1,3} ($\epsilon_{j \text{ min}} = 6B_0$) or when $\epsilon_K > 15B_0$ for rotational excitation via a dipole moment ($\epsilon_{j \text{ min}} = 2B_0$); (c) the inaccuracies of the continuous approximation for $\epsilon_K < 7kT$; and (d) the hope that a single-level approximation can eventually be solved analytically in the near-thermal region.

We will consider a homonuclear diatomic gas in which rotational excitation occurs only by the quadrupole moment ($\Delta J = \pm 2$) and in which the cross sections are given by the Gerjuoy and Stein equations.²⁶ We introduce the "single-level" approximation by assuming that only the $J=0$ and $J=2$ levels exist and that the rotational constant is B' . The cross sections for excitation and de-excitation are then^{1,2}

$$Q_{0,2} = \sigma_1(1 - 6B'/\epsilon)^{1/2}$$

and

$$Q_{2,0} = \sigma_1(1 + 6B'/\epsilon)^{1/2} \exp(-6B'/kT), \quad (A1)$$

where σ_1 and B' are to be determined. The coefficient σ_1 will be evaluated by requiring that the single-level approximation agree with the continuous approximation¹ in the limit of large electron energies. When the cross sections given above are substituted into Eq. (8) of Ref. 1 and we consider the limit of $\epsilon \gg 6B'$, then we obtain the expressions appropriate to the continuous approximation, i.e., Eqs. (10) and (11) of Ref. 1, provided that

$$\sigma_1 = (2\sigma_0/3)(B_0/B')[1 - \exp(-6B'/kT)]^{-1}, \quad (A2)$$

where $\sigma_0 = 8\pi \mathcal{Q}^2 a_0^2 / 15$ and \mathcal{Q} is the effective quadrupole moment.

We next adjust B' to give the best possible fit of the ν_u/N data calculated using Eqs. (A1) and (A2) to the experimental data for N_2 . At 77°K we find that when $kT/B' = 6 \pm 0.3$ or $B' = 4B_0$ and that the values of ν_u/N differ by less than 5% from the results of calculations^{1,3} using a full set of rotational levels for $\epsilon_K < 3kT$ and using

the various other available approximations for ϵ_K up to at least $10kT$. With the limited number of energy steps that can be used with our computer program when including collisions of the second kind, the maximum value of ϵ_K for which reliable solutions could be obtained for the Boltzmann equation is only four times that reached using the full set of levels since $B' = 4B_0$. At 293°K we find that a value of $kT/B' = 24 \pm 2$ results in values of ν_u/N for $\epsilon_K < 0.04$ eV which agree with the experimental values⁸⁷ for N_2 to within 3%. The low value of B' required at 300°K means that the single-level approximation is useful with our present computer program only for $\epsilon_K < 1.2kT$. We do not understand why the value of B' required to fit the results of the more exact analyses is essentially independent of temperature. This approximation should be tested for other gases.

In the case of rotational excitation via the permanent dipole moment, we have used an approximation in which

$$Q_{01} = \sigma_2 \frac{R_y}{\epsilon} \ln \frac{[\epsilon^{1/2} + (\epsilon - 2B')^{1/2}]}{[\epsilon^{1/2} - (\epsilon - 2B')^{1/2}]}$$

and

$$Q_{10} = \frac{\sigma_2 R_y}{\epsilon} \exp\left(\frac{-2B'}{kT}\right) \ln \frac{[(\epsilon + 2B')^{1/2} + \epsilon^{1/2}]}{[(\epsilon + 2B') - \epsilon^{1/2}]},$$

where

$$\sigma_2 = (B_0/B')\sigma_r[1 - \exp(2B'/kT)]^{-1} \text{ and } B' = (B_0 kT)^{1/2}.$$

The restriction on B' arises from the requirement that the single-level approximation agree with Eq. (7)¹ for $\epsilon \gg kT$. In order to vary B' , it is necessary to change the effective dipole moment μ from that found by fitting Eq. (7) to the experimental ν_u/N data so as to compensate approximately for the differences in the logarithmic terms introduced by $B' = (B_0 kT)^{1/2}$. As indicated in Ref. 58, a simpler approximation is now available which eliminates the difficulties encountered in trying to match the logarithmic terms in the continuous and single-level approximations.

⁸⁷ The values of ν_u/N at 293°K were calculated from the w data of J. J. Lowke [Australian J. Phys. 16, 115 (1963)] and the ϵ_K data of R. W. Crompton and M. T. Elford [in *Proceedings of the Sixth International Conference on Ionization Phenomena in Gases, Paris, 1963*, edited by P. Hubert (S.E.R.M.A., Paris, 1964), Vol. I, p. 337]. See also R. L. Jory, Australian J. Phys. 18, 237 (1965).